Digest of Translated Russian Literature

The following abstracts have been selected by the Editor from translated Russian journals supplied by the indicated societies and organizations, whose cooperation is gratefully acknowledged. Information concerning subscriptions to the publications may be obtained from these societies and organizations. Note: Volumes and numbers given are those of the English translations, not of the original Russian.

OPTICS AND SPECTROSCOPY (Optika i Spektroskopiia). Published by Optical Society of America, Washington, D. C.

Volume 12, Number 1, January 1962

Frequency Characteristics of Diffraction Modulators of Light with Ferroelectric-Ceramic Emitters of Ultrasound, I. I. Adrianova, pp. 48–51.

This paper presents results on the frequency characteristics of modulators with ferroelectric-ceramic emitters of modulated and unmodulated ultrasonic waves.

Diffraction modulators of light may be classified according to whether they use unmodulated standing waves, modulated standing waves, or traveling waves. A system of standing ultrasonic waves may be obtained by reflection, by addition of the waves from opposed emitters, or by two spatially separated traveling waves propagating in opposite directions. Accordingly, we may designate the following types of standing-wave diffraction modulators: reflection modulators, counter-emitter modulators, and double traveling-wave modulators.

In diffraction by unmodulated standing waves, the light is modulated at a frequency twice that of the ultrasound, the latter having created a diffraction grating; for diffraction by modulated standing waves the light is modulated not only at twice the frequency of the ultrasound, but also at the lower modulating frequency of the ultrasound. In the diffraction of light by a modulated traveling wave, the light is modulated only at the modulation frequency of the ultrasonic wave. A modulator of this type is called a traveling wave modulator.

In addition to these, there is still another type of diffraction modulator, the modulator-converter, based on the counter-emitter modulator. If in the counter-emitter modulator voltages at different frequencies are impressed on the emitters, then ultrasonic oscillations at these frequencies will be stored in the receptacle of the modulator, and the light in the zero-order maximum will be modulated at different frequencies. In the spectrum will occur new frequencies corresponding to combinations of the impressed high-frequency components. An analogous modulation spectrum may be obtained by using two modulators operating at different frequencies and placed in the light beam successively one after the other.

Investigation of the Plasma Jet in a Pulsed Discharge, L. I. Grechikhin, L. Ya. Min'ko, and V. E. Plyuta, pp. 60–61.

Determination of the True Contour of a Spectral Distribution from the Observed One by Using Fourier Series, B. N. Grechushnikov, p. 70.

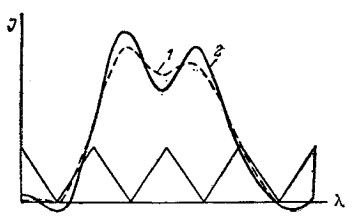

Example of reduction to the ideal apparatus. Curve 1—observed spectral distribution; curve 2 — reduced distribution.

Table 1

	$\frac{\cos x}{\sin x}$	$\frac{\cos 2x}{\sin 2x}$	$\frac{\cos 3x}{\sin 3x}$	$\frac{\cos 4x}{\sin 4x}$	$\frac{\cos 5x}{\sin 5x}$	$\cos 6x$
$N = 1/10$	1.034	1.143	1.358	1.746	2.468	3.928
$N = 1/8$	1.054	1.234	1.628	2.468	4.517	...
$N = 1/6$	1.098	1.464	2.468	5.848	...	...

It has been shown in the paper by Mandel'shtam that, when connected with a finite slit width, a triangular apparatus function of a monochromator does not distort the true spectral distribution, if it is described by harmonic functions. This fact can be used, and on the basis of it a new method convenient for practical use can be introduced, for the determination of the true contour of a spectral distribution from the observed one.

Many papers have been devoted to the latter problem (see, for example, the review in Ref. 2). Although the solution of the problem is well known in principle, the actual procedures are quite complicated for the case of an arbitrary contour, and they are not sufficiently used.

The suggested method consists essentially of the following procedures. If the spectral width of the monochromator slit is known, it is easy to find the amplitudes of harmonic components in the true spectral distribution by using the amplitude of the harmonics in the observed distribution. Fourier synthesis of these harmonics gives us the spectral distribution contour corrected for the finite width of the slits. The table gives the coefficients which are to be multiplied by the amplitudes of the harmonics in the observed spectrum, in order to obtain the true amplitudes of the harmonics for various ratios of the spectral width of the slit to the selected interval of the spectral distribution, $N = a/L$, where L is the length of the selected spectrum interval and a is half of the spectral width of the slit.

It is convenient to carry out the Fourier synthesis and analysis by means of the Beaver-Lipson strips.

The main difficulty in the reduction to the ideal apparatus is the influence of the measuring accuracy on the accuracy and inambiguity of the obtained reduction of the spectral distribution. For the reduction of higher harmonics, an increase of measuring accuracy is necessary, as it is in other methods.

As an example, the figure shows the result of the reduction of a spectrum consisting of two overlapping lines observed by means of an apparatus with a spectral slit width which is $\frac{1}{3}$ of the whole selected spectrum interval as indicated in the figure.

As should be expected, the reduction to the ideal (with respect to slit width) apparatus shows deeper maxima and minima on the curve, corresponding to a greater resolution.

References:

[1] Mandel'shtam, L. I., Collected works 1, 229 (1912) (Academy of Sciences of the USSR Press, Moscow, 1948).

[2] Rautian, S. G., "The real spectral apparatus," Uspekhi Fiz. Nauk **66**, 475–517 (1958); see references (130 titles).

Measurement of Oscillator Strengths for the Long-Wave Absorption Band of Certain Substituted Benzenes, V. I. Danilova and Yu. P. Morozova, pp. 5–7.

A systematic measurement was made of the oscillator strengths for the long-wave absorption band of 19 mono- and di-substituted benzenes containing NO_2, OH, NH_2, and COOH groups, in two solvents. Regarding the solvent as an external physical medium, we observed that the greatest agreement between theoretical and literature data was obtained by comparing oscillator strengths while taking into consideration the Lorentz and Onsager field. The relationship of oscillator strength to long-wave absorption indicates the semicomplex nature of the molecules we studied, and the existence of a definite interaction with the medium.

Deviation of oscillator strengths from the predicted values, due to specific interaction when changing from one solvent to another, can serve as a qualitative measure of this interaction. Some qualitative conclusions were arrived at, on the basis of the data obtained, concerning the relationship of oscillator strength to the nature of the group, isomer, and coupling effect.

Table 1

Substance	Solvent	n	$S \times 10^4$	$\varphi^B(n)$	f	f^A	f^B	f^m
Phenol	Water	1.372	46.94	0.841	0.053	0.074	0.041	
		1.430	45.79	0.789	0.052	0.064	0.045	...
Aniline	Hexane	1.375	16.77	0.818	0.19	0.26	0.15	...
Nitrobenzene	Hexane	1.391	87.36	0.809	0.99	1.32	0.80	
Benzoic Acid	Water	1.366	2.61	0.821	0.029	0.040	0.024	...
o-Aminophenol	≫	1.368	13.50	0.821	0.16	0.21	0.12	
m-Aminophenol	≫	1.367	7.68	0.827	0.087	0.12	0.071	...
p-Aminophenol	≫	1.364	14.04	0.820	0.18	0.22	0.13	
o-Aminobenzoic Acid	Water	1.359	11.00	0.800	0.12	0.17	0.10	
	Dioxane	1.452	23.59	0.752	0.27	0.39	0.20	0.23
m-Aminobenzoic Acid	Water	1.365	4.68	0.821	0.053	0.072	0.04	
	Dioxane	1.452	11.41	0.701	0.13	0.18	0.093	0.07
p-Aminobenzoic Acid	Water	1.381	89.42	0.812	1.31	1.40	0.80	
	Dioxane	1.462	109.56	0.755	1.24	1.80	0.95	0.41
o-Dioxybenzene	≫	1.368	8.18	0.821	0.092	0.14	0.077	
m-Dioxybenzene	≫	1.371	6.60	0.820	0.075	0.11	0.061	...
p-Dioxybenzene	≫	1.365	7.82	0.823	0.090	0.12	0.073	
o-Nitroaniline	Water	1.346	22.61	0.835	0.26	0.34	0.21	
	Hexane	1.404	15.51	0.801	0.18	0.25	0.14	0.12
m-Nitroaniline	Water	1.346	14.09	0.833	0.16	0.21	0.13	
	Hexane	1.405	10.02	0.801	0.11	0.16	0.08	0.06
p-Nitroaniline	Water	1.354	89.28	0.829	1.01	1.37	0.84	
	Hexane	1.411	56.52	0.797	0.64	0.90	0.51	0.39
o-Nitrophenol	Water	1.354	23.78	0.829	0.27	0.36	0.22	
	Hexane	1.410	22.74	0.798	0.26	0.35	0.21	0.09
m-Nitrophenol	Water	1.354	12.54	0.829	0.14	0.19	0.12	
	Hexane	1.410	11.22	0.798	0.13	0.18	0.10	0.07
o-Nitrophenol	Water	1.36	73.54	0.824	0.83	1.13	0.69	0.36

Table 2[a]

Substance	Solvent	n	$\frac{2n^2-2}{2n^2+1}$	$S \times 10^4$	$g'S \times 10^2$	$\frac{1}{\sqrt{g'S}}$	$\frac{\alpha}{r^3}$
o-Nitroaniline	Benzene 20% Benzene + 80% Heptane	1.579	0.497	29.23	33.41	1.74	...
	50% Benzene + 50% Heptane	1.410	0.397	26.44	29.10	1.84	0.56
		1.472	0.428	27.54	30.90	1.80	...

[a] Note: $g' = 3\ mc/\pi e^2 \cdot [(2n^2+1)^2/9n^3]$.

Table 3

Substance	Solvent	$\varphi^C(n)$	f^C	f^B	f^m
o-Nitroaniline	Water	0.793	0.19	0.21	0.12
	Hexane	0.682	0.11	0.14	0.12

Oscillator Strengths of Spectral Lines of Magnesium, Strontium, and Barium, N. P. Penkin and L. N. Shabanova, pp. 1–5.

The oscillator strengths of 13 lines of the principal series of strontium and barium atoms were measured by the "hook" method. It was shown that the transition probabilities in the principal series of these atoms are a nonmonotonic function of the principal quantum number at the higher levels. The oscillator strengths of the MgI and SrI lines arising from the $^3P^0_{0,1,2}$–$^3S_1$ and $^3P^0_{0,1,2}$–$^3D_{1,2,3}$ transitions were determined, as well as those of SrI and BaI lines which are produced by the simultaneous excitation of two electrons.

Table 1 f-numbers of the members of the principal series ($ns^2{}^1S_0$–$nsmp^1P^0_1$) of SrI and BaI

	SrI $5s^2{}^1S_0$–$5smp^1P^0_1$					BaI $6s^2{}^1S_0$–$6smp^1P^0_1$				
Series member	λ, Å	m	f_{rel}	f_{abs}	k	λ, Å	m	f_{rel}	f_{abs}	k
1	4607.33	5	1000	1.54	...	5535.84	6	1000	1.40	...
2	2931.83	6	3.40	0.0052	18	3071.58	7	109	0.153	21
3	2569.47	7	7.15	0.0110	18	2785.28	8	6.2	0.0087	44
4	2428.09	8	20.9	0.032	13	2646.50	9	2.22	0.0031	26
5	2354.32	9	22.3	0.034	13	2543.2	10	7.4	0.010	28
6	2307.32	10	13.1	0.020	13	2500.2	11	2.7	0.0038	25
7	2275.29	11	8.2	0.013	13	2473.20	12	0.98	0.0014	25
8	2253.32	12	4.7	0.0073	13	2452.38	13	0.11	0.00015	18
9	2237.65	13	2.8	0.0043	13	2438.81	14	0.21	0.00029	20
10	2226.38	14	1.90	0.0030	13	2427.43	15	1.30	0.0018	11
11	2217.8	15	1.34	0.0021	4	2420.11	16	0.42	0.00059	20
12	2211.3	16	1.16	0.0017	4	2414.10	17	0.19	0.00027	20
13	2206.2	17	0.81	0.0012	3	2409.25	18	0.10	0.00013	17

$\sum_{i=1}^{13} f_i = 1.64_4$ $\qquad$ $\sum_{i=1}^{13} = 1.58_4$

Table 2 f-numbers of the spectral lines of BaI due to $6s^2$–$5dmp$ transitions

λ, A	Series	m	f_{rel}	f_{abs}	k
5535.48	$6s^2\ {}^1S_0$–$6smp\ {}^1P_1^0$	6	1000	1.4	...
3889.33	$6s^2\ {}^1S_0$–$5dmp\ {}^3P_1^0$	6	6.3	0.0088	22
2702.63		7	5.1	0.0071	45
2432.54		8	1.59	0.0022	20
4132.43	$6s^2\ {}^1S_0$–$5dmp\ {}^3D_1^0$	6	6.22	0.0087	
2739.24		7	1.94	0.0027	41
2444.64		8	0.97	0.0014	20
3501.11	$6s^2\ {}^1S_0$–$5dmp\ {}^1P_1^0$	6	102	0.14	33
2596.64		7	22.2	0.031	29
2454.07	$6s^2\ {}^1S^0$–$5dmp\ {}^1P_1^0$(?)	4	0.096	0.0001	20

Table 3 f-numbers of spectral lines of CaI, SrI, and BaI due to simultaneous transitions of two electrons

Transition	Ca	Sr	Ba
$ms^2\ {}^1S_0$–$msmp\ {}^1P_1^0$	1.49	1.54	1.40
$ms^2\ {}^1S_0$–$(m-1)dmp\ {}^3D_1^0$	$43\cdot10^{-5}$	$37\cdot10^{-5}$	$870\cdot10^{-5}$
$ms^2\ {}^1S_0$–$(m-1)\ dmp\ {}^3P_1^0$	$4.3\cdot10^{-5}$	$34\cdot10^{-5}$	$880\cdot10^{-5}$

Table 4 Relative f-numbers of MgI lines arising from $^3P^0_{0,1,2}$–$^3S_1$ and $^3P^0_{0,1,2}$–$^3D_{1,2,3}$ transitions

λ, Å	Transition	j–j	f_{rel}	$\frac{\Sigma gf}{\Sigma\ gf3^3P-4^3S}$ Our data	Ref. 14	Ref. 15	Ref. 21	gf_{exp}	gf_{theor}	k
5183.60	3^3P^0–4^3S	2–1	100	1	1	1	1	100	100	65
5172.68		1–1	100					60	60	52
5167.32		0–1	100					20	20	52
3838.29	3^3P^0–3^3D	2–3	460					100	100	26
		2–2								
		2–1								
3832.30		1–2	450	4.5	6.6	3.6	4.9	62.8	60	26
		1–1								
3829.35		0–1	410					19.1	20	26
3096.90	3^3P^0–4^3D	2–3	83					91.3	100	13
		2–2								
		2–1								
3092.99		1–2	87	0.87	...	1.2	...	57.4	60	13
		1–1								
3091.08		0–1	106					23.3	20	13
2736.56	3^3P^0–6^3D	2–3	22							13
2779.83[a]	3^3P^0–$p^{23}P$	2–2	280					100	100	
2779.83[a]		1–1	94					20	20	
2782.97		2–1	99	3.8	...	4.1	5.0	35.0	33.3	13
2781.42		1–0	126					26.7	26.7	13
2776.69		1–2	160					34.6	33.3	13
2778.28		0–1	350					24.5	26.7	13

[a] The f-number is calculated on the assumption that the intensity rule is obeyed for a given multiplet.

Table 5 Absolute f-numbers of SrI lines arising from transitions from $^3P^0_{0,1,2}$ levels

λ, A	Transition	j–j	f_{abs}	f_{abs} Ref. 16	gf_{exp}	gf_{theor}	k
4607.33	5^1S–5^1P	0–1	1.54	2.2	...	...	...
7070.10	5^3P^0–6^3S	2–1	0.17	0.25	95.7	100	30
6878.38		1–1	0.17	0.24	54.8	56.8	20
6791.05		0–1	0.18	0.33	19.9	18.4	20
4962.26	5^3P^0–5^3D	2–3	0.33	0.35	98.6	100	20
4872.49		1–2	0.31	0.36	55.4	51.7	20
4967.94		2–2	0.06	0.09	17.0	17.9	20
4811.88	5^3P^0–$5p^{23}P$	2–2	0.35	0.24	94.0	100	65
4784.32		1–1	0.14	0.18	22.0	19.8	63
4722.28		1–2	0.20	0.22	31.8	32.1	66
4741.92		0–1	0.47	0.59	25.1	25.9	67
4438.04	5^3P^0–7^3S	2–1	0.029	0.035	97.7	100	8
4361.71		1–1	0.025	0.034	50.5	58.0	8
4326.44		0–1	0.034	0.036	22.9	19.0	8
3351.25	5^3P^0–$4d^{23}P$	2–2	0.17	...	90.1	100	9
3222.23		1–1	0.06	...	20.2	18.5	7
3366.33		2–1	0.06	...	32.5	33.6	9
3329.99		1–0	0.08	...	27.7	26.2	9
3307.53		1–2	0.11	...	34.5	32.4	10
3301.73		0–1	0.23	...	24.5	25.9	11

Table 6 The f-numbers of CaI, SrI, and BaI lines arising from $n^3P^0_{0,1,2}$–m^3S_1 and $n^3P^0_{0,1,2}$–$mp^{2\,3}P_{0,1,2}$

Transition	j–j	CaI, Ref. 12	SrI	BaI, Ref. 13
n^3P^0–$(n+1)^3S$	2–1	0.10	0.17	0.31
	1–1	0.12	0.17	0.36
	0–1	0.12	0.18	0.50
n^3P^0–$(n+2)^3S$	2–1	0.021	0.029	...
	1–1	0.020	0.025	0.070
	0–1	0.021	0.034	0.079
n^3P^0–$np^{23}P$	2–2	0.29	0.35	0.26
	1–1	0.11	0.14	0.28
	2–1	0.10	0.13[a]	0.29
	1–0	0.14	0.17[a]	0.27
	1–2	0.17	0.20	0.25
	0–1	0.40	0.47	0.94

[a] The f-number is calculated on the assumption that the intensity rule is obeyed for a given multiplet.

Volume 12, Number 2, February 1962

Multiconfigurational Approximation and Its Convergence, A. P. Yutsis, Ya. I. Vizbaraite, T. D. Strotskite, and A. A. Bandzaitis, pp. 83–86.

The mathematical basis for the multiconfigurational approximation is a generalization of the Ritz method; not only the coefficients of the basic functions are varied but also the functions themselves. The basic functions determined in this fashion guarantee rapid convergence of the method. Any deviation from these functions weakens the convergence. It has been shown that the sum of the energy corrections, obtained from the separate two configurational approximation for atoms of the helium type, gives the full correction if only the configurations of equivalent electrons are used as corrective configurations. For atoms of the beryllium type the sum of the corrections for the separate shells gives a correction to the multiconfigurational approximation for the whole atom. Preliminary results of calculations for atoms of the helium and beryllium type show that both the wave function and the energy obtained from the multiconfigurational approximation, based on a generalization of the Ritz method, converge rapidly toward the solution, and, correspondingly, toward the eigenvalue of the Schroedinger equation.

Some Distortions in Fourier Spectrometry, B. A. Kiselev and P. F. Parshin, pp. 169–172.

The fundamental equation of Fourier spectrometry is derived. By analysis of this equation the dependence of the real resolution, intensity, and amount of line shift in a particular spectrogram on the dimensions of the exit aperture of the interferometer is determined for cases of finite and infinite path difference. The treatment is based on models of lines described by a δ-function and a dispersion curve.

Concentration of Charged Particles in the Plasma of an Arc Burning in an Atmosphere of Argon and Helium, V. F. Kitaeva, V. V. Obukhov-Denisov, and N. N. Sobolev, pp. 94–98.

The contours of H_α, H_β, H_γ, and H_δ are measured in 1–200 amp arcs burning in argon and helium. The experimental contours are compared with theoretical contours calculated by Griem, Kolb, and Shen. Satisfactory agreement is obtained between theory and experiment. Comparison of the experimental and theoretical contours permits determination of the concentration of charged particles in arcs burning in argon (2×10^{14} to 3×10^{16} cm^{-3}) and helium (4×10^{13} to 2×10^{16} cm^{-3}) at currents of 1 and 6 to 200 amp, respectively. The low concentrations of charged particles existing in these arcs at low currents appear to be one of the basic causes of the nonequilibrium population of the levels.

Polarization of Fluorescence and Spectral Classification of Complex Molecules, V. P. Klochkov and B. S. Neporent, pp. 125–128.

The change in the degree of fluorescence polarization in the fluorescence and absorption spectra of several compounds, whose spectra consist of broad structureless bands, has been studied. It has been shown that the change in the degree of polarization in the fluorescence spectrum, observed in a number of instances, is connected with the presence of at least two luminescence centers, which differ in their degree of fluorescence polarization.

Experimental Study of Circular Dichroism and Optical Activity of Sodium Uranyl Acetate Single Crystals, M. S. Brodin and Ya. O. Dovgii, pp. 155–157.

Absorption spectra of sodium uranyl acetate single crystals were obtained at low temperatures. Seven lines were found, arranged in a characteristic fashion and exhibiting a high degree of circular dichroism. Absorption coefficient curves corresponding to several bands of crystalline origin observed at 20°K were plotted for d- and l-rotary crystals. The data obtained concerning the spectral distribution of optical activity show that a sodium uranyl acetate crystal rotates the plane of polarization to an appreciable extent only in the neighborhood of bands exhibiting marked circular dichroism.

Absorption Spectra of Glasses of the System As_2S_3–As_2Se_3, A. Vashko, G. Prokopova, B. T. Kolomiets, B. V. Pavlov, and V. P. Shilo, pp. 149–150.

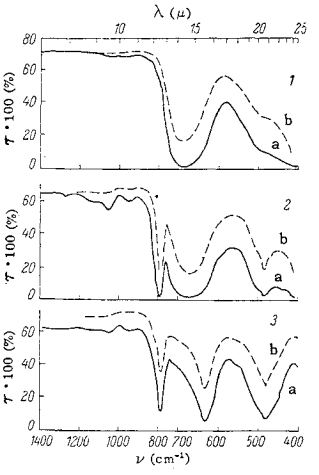

Fig. 1 The optical absorption of As_2S_3 (1), As_2S_3·As_2Se_3 (2), and As_2Se_3 (3). Thickness of samples (in mm): 1—0.63 (curve a), 0.28 (curve b); 2—0.66 (curve a), 0.24 (curve b); 3—0.48 (curve a), 0.19 (curve b). In the 400–700 cm^{-1} region the abscissa scale is expanded to double that used in the 700–1400 cm^{-1} region.

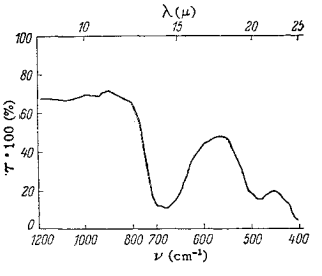

Fig. 2 The optical absorption of the As_2S_3·As_2Se_3 sample prepared in the gas-free tube. Thickness of 0.53 mm; in the region 400–700 cm^{-1} the abscissa scale is expanded to double that used in the 600–1200 cm^{-1} region.

In other papers dealing with the optical properties of vitreous semiconductors, the absorption spectrum of the system As_2S_3-As_2Se_3 was investigated up to 18μ. Elsewhere the absorption spectrum of vitreous As_2S_3 was measured up to 25μ. The present investigation was aimed at providing a more detailed knowledge of the absorption spectra of the forementioned glasses up to 25 μ and at determining the wavelengths of all of the absorption bands.

Determination of the Microcharacteristics of Copper from Its Infrared Optical Constants and Its Conductivity at 82° and 295°K, V. G. Padalka and I. N. Shklyarevskii, pp. 158–162.

The indices of refraction and absorption of thick copper films obtained by vacuum deposition were measured at wavelengths between 1 and 12μ. The conductivity of the same samples was determined at 82° and 295° K. A connection was made for the effect of oxide films formed on the surface of the copper. The concentration of conduction electrons was determined, as well as their velocity at the Fermi surface; the frequencies of electron-electron, electron-phonon, and electron-impurity collision were also measured. The results are compared with the data based on measurements of electronic specific heat and surface impedance at radio frequencies.

Transmission of Light through a Transparent Uniaxial Crystal Plate, F. I. Fedorov and T. L. Kotyash, pp. 162–164.

The polarization of a transmitted wave is calculated rigorously for light incident normally on a plane-parallel plate cut from a transparent uniaxial crystal, the orientation of the optical axis being arbitrary. Reflections from both surfaces are taken into account. It is shown that the conventional calculation, which considers only the phase difference between the ordinary and

extraordinary waves emerging from the plate, may lead to an appreciable error in the determination of the polarization of the transmitted wave.

Diffusion of Light in Scattering Media, Yu. A. Tsirlin, L. E. Pargamanik, and A. R. Daich, pp. 165–168.

The propagation of light through a layer of scattering and absorbing material is investigated with the aid of a diffusion approximation. The method of calculation makes it possible to study problems with complex geometry. Calculations for plane and point sources are confirmed by experiment.

Volume 12, Number 3, March 1962

Dependence of Spectral Line Intensities on the Effective Ionization Potential of the Arc, V. L. Ginzburg and N. P. Glukhovetskaya, pp. 190–193.

The intensities of spectral lines of different elements in a carbon arc were studied as a function of the quantity of alkali metal introduced into the arc. It is shown that this dependence obeys the same law as the dependence of spectral line intensities on arc temperature calculated theoretically by Mandel'shtam. It is further shown that spectral lines of different elements are not necessarily homologous if their excitation potentials are equal.

Spectral Study of CdS- and CdS,CdSe:Colored Glasses, I. M. Buzhinskii and N. I. Bodrova, pp. 212–217.

The absorption spectra (in the region 300–700 mμ) and the luminescence spectra were studied for a group of specially fused glasses of a single basic composition with various percentages of Cd, S, and Se. The pattern of spectral changes at various temperatures of heat treatment is presented in detail as a function of the relative content of Cd, S, and Se. For a Cd content insufficient for complete bonding of all S and Se atoms, a complex pattern of spectral changes was observed, differing as a function of the excess of S or Se relative to Cd. Ideas of solid state physical (formation of "impurity" levels) are offered for its explanation.

Passage of Light through Plates of Uniaxial Optically Active Crystals Belonging to Axial Classes. I. General Solution, F. I. Fedorov and A. F. Konstantinova, pp. 223–225.

The passage of a light wave through a plane-parallel plate made of an optically active crystal belonging to the axial class of central syngonies is rigorously analyzed. Normal incidence of light is considered, with arbitrary orientation of the optic axis. Explicit expressions are derived for the amplitudes of the transmitted wave in terms of the amplitudes of the incident wave, with account being taken of reflection from both faces of the plate.

Coherent Scattering of Light in Glass, N. A. Voishvillo, pp. 225–229.

A study is made of the scattering of light by glass in which it is necessary to take into account the interference of radiation scattered by different glass inhomogeneities. We use a theory analogous to the theory of scattering of x rays. We compute the radial correlation function which characterizes the structure of the glass. On the basis of the analytic representation of the correlation function obtained, we compute the scattering indicatrices which agree satisfactorily with the experimental values, including the "anomalous" ones.

High Light-Speed Electron-Optical System for Spectral Investigations of Plasma, M. M. Butslov, A. G. Plakhov, and V. V. Shapkin, pp. 229–231.

The electron-optical system investigated in the present paper consisted of the simplest electron-optical image converter with electrostatic focusing and a magnetic quadrupole lens. It is shown that such a system is capable of changing within wide limits the scale of the electronic image along two mutually perpendicular axes while retaining good image quality. Such a system is very efficient for spectral investigations of weakly luminescing plasma.

Optical Method for Filtering the Green Line of Hg^{198}, N. R. Batarchukova, A. I. Kartashev, and A. P. Kirichenko, pp. 232–233.

This paper describes methods for the narrowing of the spectral lines of Hg^{198} using resonance absorption. Arrangement for a "Zeeman absorption filter" for the narrowing of resonance lines and for a "heat absorption filter" are described. Using the latter, it was possible to reduce the width of the Hg λ 0.5461 μ line emitted by an electrodeless Meggers-type lamp which was cooled to a temperature of 15°C by a factor of approximately 1.5–2. An interference pattern of fringes of equal inclination was obtained with a path difference of 750 mm in a Fabry-Perot etalon.

Theory of Optical Signal Amplification by a Medium with Negative Absorption, Yu. M. Kagan, V. I. Perel', and M. P. Chaika, pp. 234–237.

A study is made of the amplification of an optical signal by a medium with negative absorption. The use of mirrors to increase the coefficient of amplification is considered in the following cases: ideal mirrors; practical mirrors with surface irregularities and finite dimensions. The frequency distribution of the amplified signal is given for initial line contours of the Doppler and Lorentz types.

Reflection and Transmission of Light by Plane-Parallel Layers with a Negative Absorption Coefficient, B. I. Stepanov, pp. 242–243.

Volume 12, Number 4, April 1962

Semiempirical Method for Calculating the Oscillator Strengths of Intercombination Transitions, L. A. Vainshtein and I. A. Poluektov (pp. 460–465), pp. 254–257.

The complete matrix of spin-orbit and spin-spin magnetic interactions is calculated for the *sl* configuration, assuming intermediate coupling. The results obtained are used to compute the relative oscillator strengths of intercombination and permitted optical transitions in divalent elements. The radial integrals are evaluated by a semiempirical method. The relationship between the formula obtained and the well-known Pauli-Houston formula is discussed.

Mechanism of the "Carrier" Effect on the Intensity of Spectral Lines, Z. N. Samsonova, pp. 257–261.

An investigation of a series of "carriers" has been undertaken. The extent to which they affect the intensity of spectral lines directly through evaporation of the constituents and indirectly through influencing the conditions which obtain in the plasma of the arc column has been clarified. The evaporation of the sample containing "carriers" results in a positive effect on the lines for only a small number of constituents. On the other hand, the conditions of discharge which are realized in the presence of "carriers" affect favorably the lines of most of the constituents in the sample. This results from an increase in the integral concentration of atoms in the analytical volume of the plasma.

Use of Fraunhofer Diffraction for Measuring Light Dispersion, V. G. Khomazyuk, pp. 277–279.

The phenomenon of Fraunhofer diffraction, in an aperture half closed by a transparent plane-parallel plate, is investigated in this article. A simple high-illumination method for determining the light dispersion in the whole photographic region of the spectrum is proposed.

Passage of Light through Plates of Uniaxial Optically Active Crystals. II. Plates Cut Parallel to the Optic Axis, F. I. Fedorvo and A. F. Konstantinova, pp. 280–282.

This paper deals with the polarization of light transmitted along a normal through a plate of uniaxial optically active crystal of the axial class, cut parallel to the optic axis, and also deals with the case of transmission through two such crystals with axes crossed. It is shown that in this case no rotation of the plane of polarization of the light occurs, even approximately.

Determination of the True Contour of a Spectral Line from the Observed Contour, A. F. Bondarev, pp. 282–284.

A method is proposed which permits the determination of the true contour of a spectral line from the observed contour, provided that the contours are symmetrical. The method is applied to Raman lines. Numerical results are given.

Thermodynamic Calculation of the Concentration of Metal Atoms and Flame Temperature, N. S. Tskhai, pp. 291–292.

In a previous paper, we investigated the causes of the changes which occur in the intensities of spectral lines of Na and Sr in an acetylene-air flame as a function of the compounds used and the other compounds present in the solution. The concentration of atoms in the flame was measured by the dispersion method; the flame temperature was measured by the reversal method, using the lithium line. It was established that the observed

changes in line intensities occurred because of the simultaneous effect of two factors—the change in the concentration of free atoms of the elements studied in the flame and the change in flame temperature. It was further established that for sodium the change in the concentration of atoms in the flame occurred because of the change in the rate of introduction of solution into the flame with changing composition; the same effect occurs for strontium. There is more to it than this, however; there must be other factors influencing the change in concentration of strontium atoms in the flame as a function of the form of the compound used and the presence of "third" elements.

We wished to obtain a more complete idea of the probable causes of the change in atomic concentrations in the flame and to investigate the possibility of changes in flame temperature occurring as the result of shifts in the thermal equilibrium of chemical reactions taking place in the flame. We therefore performed thermodynamic calculations of flame temperature and atomic concentration of Na and Sr when introduced into the flame as solutions of chloride salts, with and without additional solutes. The results of these calculations were compared with experiment.

Volume 12, Number 5, May 1962

Collision of Slow Electrons with Hydrogen Atoms, V. D. Kamenetskii, p. 366.

In another paper, a simple quantum-mechanical method, using trial wave functions, was suggested for calculating collisions of slow particles. Its parameters were determined without recourse to variational methods. Various special applications of this method were studied in detail elsewhere. In the present communication we give the results of calculations of the elastic scattering of S-electrons by hydrogen atoms without considering exchange; the calculations were carried out by one of the most promising modifications of the new procedure—that involving self-consistency at the boundary.

The method of self-consistency at the boundary is a direct generalization of the method of series expansion and of the method of asymptotic self-consistency. The parameters of the trial functions are determined in this method by considering the behavior of the trial functions at $r \to 0$ and $r \to \infty$.

Volume 12, Number 6, June 1962

Continuous Emission Spectra of Krypton and Xenon behind a Shock Wave, A. P. Dronov, A. G. Sviridov, and N. N. Sobolev, pp. 383–389.

Kantrowitz and his collaborators have investigated the continuous emission spectrum of argon behind a shock wave for Mach number values of 11.2 to 16.8 (equilibrium temperature 10,300–13,700°K) and have found that the measured brightness is in satisfactory agreement with the value predicted by the Kramers-Unsöld recombination theory. Experimental data on the energy distribution in the continuous spectrum of electrical discharges in inert gases are also in satisfactory agreement with the recombination theory.

Roth and Gloersen have also pointed out another possible cause for the production of a continuous spectrum behind relatively weak shock waves in inert gases. Using a photoelectric method, they studied the emission spectrum of xenon behind a shock wave at M values between 8 and 11 (equilibrium temperature 6000°–9000°K). In interpreting their experimental results, they used the results of Tanaka, who had demonstrated the existence of xenon quasi-molecules Xe_2^*. According to Roth and Gloersen the continuous xenon emission spectrum is produced under their experimental conditions as a result of a transition of the xenon molecule from an excited stable state to an unstable ground state, followed by dissociation.

Despite the very considerable amount of experimental work performed by Roth and Gloersen, the interpretation of their results is not unequivocal. In particular, it may be that for M values of 10–11 (T = 8000°–9000°K) the basic mechanism leading to the emission of a continuous spectrum behind a shock wave in xenon is still the recombination of ions and electrons, because under these conditions the equilibrium concentration of charged particles is greater than 10^{16} cm^{-3}, i.e., high enough to guarantee an intense recombination radiation. The observed delay, which is very important according to Roth and Gloersen, can be related to the finite time necessary for the establishment of ionization equilibrium.

In one way or another, at least two mechanisms can be mentioned at present which would lead to the emission of a continuous spectrum behind a shock wave in inert gases. It is therefore necessary to keep both of these mechanisms in mind when planning and interpreting experiments.

The present paper describes an investigation of the continuous spectra of krypton and xenon behind a shock wave between M values of 11.5 and 15, that is, at M values which are higher than those in Roth and Gloersen's experiments. Even if Roth and Gloersen's mechanism is correct, its contribution to the continuous spectra of inert gases should certainly decrease as the velocity of the shock wave (and the concentration of charged particles) increase. On the other hand, the role of the recombination mechanism should increase. Starting from this point, we have tried to interpret our experimental results on the basis of the Kramers-Unsöld recombination theory, a discussion of which, as applied to krypton and xenon, is given prior to the description of the apparatus and the presentation of results. Strictly speaking, the Kramers-Unsöld theory is valid only for hydrogen. Its application to inert gases is based on the fact that the excited levels of noble gases are more hydrogenlike than the excited levels of other elements.

Rotational Diffusion of Molecules and the Scattering of Light in Liquids. I. Spherical Molecules, K. A. Valiev and L. D. Eskin, pp. 429–432.

Diffusion processes have long been, and continue to be, the subject of a constantly growing number of investigations in both mathematical and experimental physics. The most detailed studies have been made in the theory of processes of progressive diffusion of particles—molecules, neutrons, and photons—in connection with important applications of this theory. Rotational diffusion processes of particles (molecules or complexes of molecules) have not received such an extensive theoretical treatment; still, such processes determine the character of a wide variety of phenomena—Rayleigh and Raman scattering of light, dielectric relaxation, paramagnetic relaxation, and resonance, etc. In studying these phenomena, one usually employs an equation for the rotational diffusion of a linear molecule, and describes its orientation in terms of two spherical angles which correspond to the two rotational degrees of freedom.

This paper deals with the diffusional rotation of a spherically symmetrical molecule. Such a molecule possesses three rotational degrees of freedom, which are described by the Eulerian angles θ, ψ, and φ. In order to conduct this investigation, one must use the group theoretical formalism based on the representations of the three-dimensional rotational group. Starting from the Fokker–Planck equation, we find an equation for hindered rotational diffusion, which represents a generalization of the previously known equation for rotational diffusion of a linear molecule. A solution of this equation (the transition probability) is given in the form of an expansion in terms of generalized spherical functions. The subsequent sections are devoted to the application of these results to the scattering of light in liquids. The authors plan the development of methods suitable for the extension of the results of this paper to nonspherical molecules.

Sensitivity of the Radiant Point Method, III. M. A. Vorob'eva, pp. 433–434.

Obreimov has calculated the visibility of the shadow produced by an inhomogeneity in refractive index of the following type in an infinite medium (for example, a plane parallel plate): Region I has the refractive index μ_1, and region II the refractive index μ_2; regions I and II are separated by a transition region in which the refractive index varies linearly from μ_1 to μ_2. However, Obreimov assumed that region II is wide (that is, it extends over several Fresnel zones). In the present paper we do not make this assumption.

On the Paper "The Absorption Spectra of Neodymium Chloride in Alcohol-Water Solutions at Low Temperatures," A. N. Zaidel, p. 456.

We have previously shown that the addition of small amounts of water to alcoholic solutions of neodymium chloride causes a gradual change in the spectra, which was explained by the simultaneous existence in the solution of alcohol- and water-solvates of the neodymium ion. This point of view has been subjected to criticism by Pominov, who, on the basis of his results, came to the conclusion that in these solutions there existed mixed alcohol-water solvates. Our measurements were conducted near the freezing point of alcohol, whereas Pominov was investigating the spectra at room temperature. A comparison of the results of the

two investigations is not particularly easy, since the conditions of formation of a particular solvate may change appreciably with temperature. In following up our work, Pominov carried out his measurements at low temperatures and confirmed our old results, although he did not feel it necessary to state this sufficiently clearly in his article.

Let us try to compare the results of all these investigations in order to explain the state of the question concerning the existence in solution of different types of solvates. At low temperatures there exist only pure alcohol or water solvates. This follows from our investigation, and is now confirmed by Pominov. At room temperature, according to our data, there still exist only pure solvates, whereas Pominov admits the simultaneous existence of both aqueous and mixed solvates. Without having sufficient basis to deny this point of view, since the fundamental experiments were carried out by us at a temperature of −80°C, we can only indicate that it is in contradiction not only with our experiments which were carried out at room temperature, but also with the data of earlier investigations on the absorption spectrum of europium.

Volume 13, Number 1, July 1962

Effect of Nuclear Quadrupole Moments on Forbidden Transitions in Hydrogen-Like Atoms, L. A. Borisoglebskii, pp. 1–5.

In 1935, Schüler and Schmidt first suggested an effect of the nuclear quadrupole moment on atomic spectra (and also the existence of such a moment), when they were studying the hyperfine structure of the europium spectrum. The exact quantum theory of the quadrupole interaction between the nucleus and orbital electrons then formulated was successfully applied to determine nuclear quadrupole moments from the experimental hyperfine structure data of various spectra. Since the Bohr frequencies corresponding to the differences between hyperfine structure levels of the same fine structure term fall in the radio-frequency spectrum, the magnetic resonance method could be used to determine these levels, and hence also the nuclear quadrupole moments. This method has, in fact, given the most accurate values of the nuclear quadrupole moments of various elements.

However, the interactions of nuclear moments, both quadrupole and magnetic, with the orbital electrons do not only affect the hyperfine structure of the atomic levels. General quantum mechanical considerations show that these interactions must also lead to forbidden atomic transitions. Theory and experiment have shown that nuclear magnetic interaction is responsible for some of the forbidden lines of mercury and cadmium (λ 2655.58 Å, $6s^2\ {}^1S_0 \rightarrow 6sp\ {}^3P_0$, Hg I; λ 3320 Å, $5s^2\ {}^1S_0 \rightarrow 5sp\ {}^3P_0$, Cd I, etc.). So far as the present author knows, the effect of the nuclear quadrupole moment on forbidden lines has never been considered.

In the present paper, we consider the effect of the nuclear quadrupole moment on forbidden transitions in hydrogen-like atoms. The calculations use the perturbation method in a non-relativistic approximation. In the first section we examine some of the properties of the operators for quadrupole and magnetic interactions and we establish selection rules for various transitions (dipole as well quadrupole and magnetic) induced by these interactions. Section II is devoted to a computation of the relative and absolute probabilities of forbidden dipole transitions.

Mechanism of the Formation of Equilibrium Concentration of the Electrode Material in the Plasma of the Arc Discharge, I. M. Belousova, pp. 6–10.

The mechanism of the formation of equilibrium concentration of the electrode material entering the plasma of an arc discharge was studied. For this purpose, the plasma of the d.c. arc was transformed for a short period of time from one state into another by superimposing on it an additional current pulse. A decrease of concentration of the electrode material was found with the decrease of pressure of the discharge. This decrease of concentration is connected with the shortening of the time the particles remain in the discharge zone. The formation of the equilibrium spatial distribution of particles, which is characterized by a sharp gradient of the material concentration at the plasma "boundary," takes place in a time of the order of 10^{-4} sec.

Temperature and Thermal Equilibrium in the Arc Burning in Inert Gases, R. R. Shvangiradze, K. A. Oganezov, and B. Ya. Chikhladze, pp. 14–17.

The spectrum of a 10-amp d.c. arc burning between pure graphite electrodes was studied in nitrogen, argon, helium, neon, and krypton. In arc burning in inert gases, the spectra of CN, Fe I, Fe II, C II, C III, and lines of noble gas atoms and ions with excitation energies up to 23–24 ev are excited simultaneously. Essentially no difference was observed between spectra produced by pure graphite electrodes and those produced between electrodes that were contaminated with iron. The iron atoms and ions showed a thermal distribution of excitation levels; the same was true of the vibrational states of the CN molecules. The relative intensities of CN bands ($\Delta v = 0$ and $\Delta v = -1$) and Fe I, Fe II, and C II lines, as well as the Doppler broadening of the Fe I line (T_D), were used in temperature measurements. The temperature values obtained were related to each other as follows:

$$T_{CN} < T_{FeI} \lesssim T_D \lesssim T_{FeII} \ll T_{CII}$$

Breakdown of a One-to-One Correspondence between Image and Object, D. Yu. Gal'pern, pp. 67–69.

It is shown that different self-luminous and nonself-luminous objects under certain conditions lead to completely identical images. Therefore, generally speaking, it is not possible unambiguously to determine the amplitude distribution in the object plane using a known image.

Conclusion: It has been shown that several different self-luminous, as well as nonself-luminous, objects under certain conditions give strictly identical images. Therefore, in the general case it is not possible by any means (for example, by calculation) to reconstruct from a known image the distribution of luminosity or amplitude in the object plane. The proofs carried out in this article, strictly speaking, do not refute the statements of Tsybakov, Yakovlev, and Wolter, since the latter assumed that the object was bounded, whereas infinite objects are considered in the proof of the theorems of Ignatovskii. However, the practical view of any apparatus, measured in optical units, is almost infinite. For example, the field of view of a microscope is 1000–1500 optical units. Making use of the present-day terminology of image theory, we can say that the periodic components in an analysis of the function which gives the distribution of luminosity or amplitude in the image plane lead to a uniform background if the period is less than π in the case of an incoherent object and less than 2π for a coherent object.

Enhancement of the Resolving Power of Telescope Systems Relative to Two Point Sources of Greatly Different Intensity, A. N. Ryazanov, pp. 70–71.

A criterion for the resolution of two light sources of greatly different intensity is formulated for a simple circular objective. Calculations are carried out for objectives which substantially reduce the intensity of the diffraction rings near the central maximum, and a possible application of such objectives is considered.

Relativistic Treatment of Radiation Transitions, F. A. Babushkin, pp. 77–78.

Possibility of Enhancing the Sensitivity of the Fourier-Spectrometry Method, B. M. Golubitskii, pp. 83–84.

Volume 13, Number 2, August 1962

Method for the Calculation of a Multilayer Coating with a Given Reflectivity, A. M. Ermolaev, I. M. Minkov, and A. G. Vlasov, pp. 142–146.

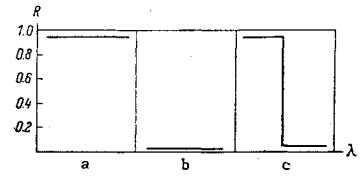

Fig. 1 Examples of optical filters: a) interference mirror; b) antireflection coating; c) cutoff filter.

Let us consider a coating consisting of N layers whose reflectivity R_N is given by

$$R_N = R_N(x_0, x_1, \ldots x_N, x_{N+1}, \vartheta, \lambda)$$

In Eq. (1) x_0 and x_{N+1} are the optical constants of the media on either side of the coating x_j (where $j = 1, 2, \ldots N$) are the optical parameters of the jth layer in the coating, ϑ is the angle of incidence, and λ is the wavelength of the incident light. In the case of systems consisting of flat isotropic layers x_j will consist of three quantities, namely, the refractive index n_j, the

absorption coefficient κ_j, and the film thickness h_j.

Because of the existence of a specific relationship between the reflectivity of a given coating and λ it is possible to use multilayer coatings to change the spectral composition of a light beam. Thin film systems deposited onto a suitable "substrate" are used as reflectors (interference mirrors), antireflection coatings, and for the separation of light beams (interference filters and cutoff filters). The action of these optical systems is illustrated in Fig. 1.

In order to construct coatings for one of the forementioned purposes the following problem has to be solved: the number of layers N and the values of the parameters $x_1, x_2, \ldots x_N$ have to be determined for which the reflectivity $R_N(\lambda)$ in the wavelength region of interest ($\lambda_2 \geqslant \lambda \geqslant \lambda_1$) and for a fixed angle of incidence ϑ is equal to the given function $F_0(\lambda)$:

$$R_N(x_1, x_2, \ldots x_N, \lambda) = F_0(\lambda) \qquad (2)$$

The most interesting of all the known publications on the design of multilayer coatings is the paper by Baumeister; an approximate method for the solution of this problem is described which is based on passing from Eq. (2), which is nonlinear in x_j, to the study of certain linear systems. We will not examine in detail the method of refinement described in that paper. We shall point out only that "localization" is its essential feature: the initial coating can be improved only when all the optical thicknesses d_j' of the "refined" version of the coating differ only by very little from the optical thicknesses d_j of the initial coating (the refractive indexes were not varied in this method).

In the present work we shall present an efficient numerical method for the design of multilayer coatings with a given reflectivity $R(\lambda)$ which is based on the use of an electronic computer. Unlike the method of Baumeister, the method described here is not strongly localized. This results in greater freedom in the variation of the layer parameters for the choice of their optimum values.

Spatially-Limited Total-Internal-Reflection Resonance Filter. II, L. V. Iogansen, pp. 146–148.

The characteristics of a spatially limited total-internal-reflection filter are calculated for the case of p-polarization of electromagnetic waves. Results qualitatively agree with expressions obtained earlier for the characteristics of a filter in the case of s-polarized waves.

Multilamp Source of Modulated Light for a Pulse Taumeter, N. A. Tolstoi and M. V. Epifanov, pp. 162–164.

The use of the pulse taumeter in the investigation of luminescence spectra of monomolecular luminors with linear spectra has made it possible to study several substances with a greater detail than ever before. The number of research problems in which this method will undoubtedly be used is very large, particularly because of the increasing interest in crystalline quantum generators of light. The new light modulator described here makes a substantial improvement possible in the pulse taumeter method.

The chief inconvenience of the pulse taumeter in comparison with the usual taumeter, in which periodic rectangular pulses of the exciting light are used, is the fact there is only a single light pulse which excites the process being studied. Besides the fact that an oscilloscope with a long-persistance screen is always less convenient and less precise than an oscilloscope with a stationary pattern on a normal screen, the necessity of choosing values of RC which "linearize" the taumeter loop slows the measurement process considerably because of the many trials needed. The conversion of a pulse lamp to a periodic regime with a sufficiently large frequency of pulse repetition while maintaining the pulse energy is not possible in the majority of cases because of thermal overloading of the lamp.

The forementioned drawbacks of the single-pulse taumeter are completely removed by using the multilamp light modulator which we have developed (Fig. 1).

Vibrational Spectra of Cyanamide, Yu. I. Mushkin and A. I. Finkel'shtein, pp. 161–162.

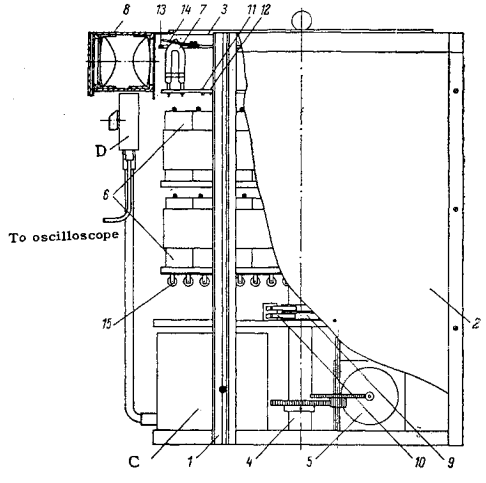

Fig. 1 Diagram of the multilamp pulsed source of light; 1—frame; 2—housing; 3—cover; 4—axis with platforms for mounting of capacitors and lamps; 5—motor (SD-09) with reduction gears; 6—capacitors (1300 μf, 300 v); 7—IFK-120 lamps; 8—parabolic quartz condenser (K); 9—rotating ring contacts (RC); 10—stationary contacts (SC); 11—contacts for firing electrode of IFK-120 lamps (CNT-1); 12—contacts for ignition of IFK-120 lamps (CNT-2); 13—support for lamp-positioning plate; 14—lamp-positioning plate; 15—resistors (R) in capacitor charging circuits. See Fig. 2 for C and D.

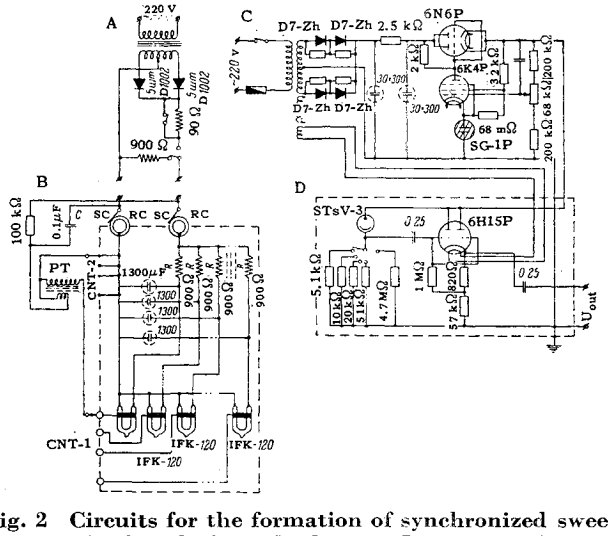

Fig. 2 Circuits for the formation of synchronized sweep pulses: A—Supply for pulse lamps; B—circuit of pulsed light source; C—supply for cathode follower; D—photoelement and cathode follower.